Retinal Image Biometric Coding using a Logarithmic Spiral and a Time Series Representation

Fabiola M. Villalobos-Castaldi[1], Edgardo M. Felipe-Riverón[2]

[1,] *Center of Research and Advanced studies of the National Polytechnic Institute Av. IPN # 2508 Col. Instituto Politécnico Nacional s/n, La Laguna Ticoman, Gustavo A. Madero, Mexico City, D.F., 07360, Phone: (52)- 55 5747 3800/6211*
[2,] *Center for Computing Research, National Polytechnic Institute, Av. Juan de Dios Batiz and Miguel Othon de Mendizabal, Mexico, D.F., P. O. 07738. Mexico, Phone: (52)-55-5729 6000/56515.*
[1]*mvillalobos@cinvestav.mx,* [2] *edgardo@cic.ipn.mx*

Abstract. The retina has many desirable characteristics as a basis for authentication, including uniqueness, stability, and permanence. In this paper, we propose a new approach for retinal images feature extraction and template coding. The use of the logarithmic spiral in scanning and tracking the vascular network, and the time series technologies such as SAX representation conform the key to make this new approach simple, flexible and reliable. Experiments show that this approach can achieve the reduction of data dimensionality and of the required time to obtain the biometric code of the vascular network in a retinal image.

Keywords: Biometric code, logarithmic spiral scan and tracking, time series, retinal images.

Introduction

It has been proposed a number of authentication methods based on the retina. These methods have focused primarily on selecting the appropriate features to represent the retina (bifurcations, ending points, etc.). But the final representation of the features has never been studied carefully. Biometric representation (*template*) is a machine readable and understandable form of a biometric trait. It influences the system's accuracy and the design of the rest of the system. The machine representation of a biometric is critical to the success of the matching algorithm. In a practical authentication system, the database can contain records of millions of people. Choosing an appropriate representation of the features in order to make the database smaller in size, having a rapid response search and while retaining high accuracy in the verification, is a vital task.

From previous studies, the retina's features used for authentication can be classified into three main categories: structural, statistical and algebraic features. Some typical structural features include main lines (centerlines), branching points,

Advances in Computer Science and Engineering
Research in Computing Science 58, 2012 pp. 91–108
Paper Recived 01-10-2012 and Acepted 07-11-2012

crossing points, termination points, positions, angles, diameters, etc. Some statistical features are the texture moments and the random values. Likewise, the algebraic features, such as band-tree based radial partition, the ring method, etc.

The main contribution of this paper will be the implementation of a new biometric representation method based on coding blood vessel segments, through a new scanning and tracking algorithm of a logarithmic spiral type, from which is obtained a time series representation of the local features of the detected and analyzed segments. The time series have been studied extensively in data mining, bioinformatics and pattern recognition in biometrics [1].

Disadvantages of the actual sampling methods

There are several disadvantages that the actual sampling methods have when they are applied to retinal images. [1]-[16]. These are:

- The retina has an average of 400 minutiae points, between bifurcation, intersection and ending points, thus the point to point comparison for all the retinal images contained in a database is impractical and computationally expensive.
- To encode a minutiae, it is necessary to perform an image preprocessing step, within which is included retinal network thinning, which presents a problem because most existing thinning methods, if not all, create false positives when converting an intersection in a double crossing point and breaking segments; this problem generates a greater number of ending points than those that actually exist in the original image [28-32].
- To make the method more robust, it is necessary to extract additional information from the detected minutiae such as angles, distances between the minutiae and the reference point (center of the optic disc), minutiae distance, etc., that increases the required processing time [33].
- The minutiae-based encoding method does not use the retinal vascular network structure properties that are essentially the most robust and stable of all characteristics [34-35].

Logarithmic spiral

A spiral is a curve that winds itself around a certain point. While not being a circle, the radius will vary along the angle [20], [21]. The logarithmic spiral is the spiral for which the radius grows exponentially with the angle. The logarithmic relation between radius and angle leads to the name of **logarithmic spiral**. In this curve the distances where a radius from the origin meets the curve increases in geometric progression.

The logarithmic spiral is a spiral whose polar equation is given by:

$$r = \qquad \text{(Eq. 1)}$$

where r is the distance from the origin, θ is the angle from the x-axis, and a and b are arbitrary constants. The constant a is the rate of increase of the spiral. The sign of a determines the direction of rotation of the spiral. The logarithmic spiral is also known as the growth spiral, equiangular spiral, and spiral mirabilis. The logarithmic spiral is remarkable because of its unique self-similarity; it is invariant after a similarity transform. After any scaling (uniformly increasing or decreasing the size), logarithmic spirals can be rotated such that they match the original figure.

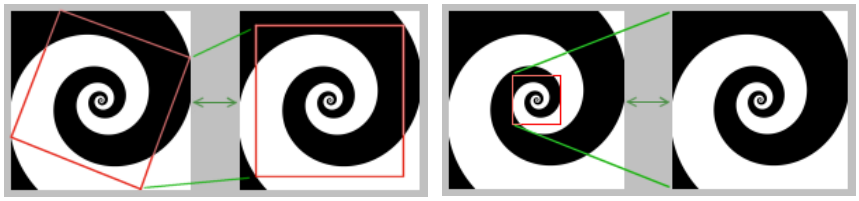

Fig. 1 Self-similarity of the logarithmic spiral

The spiral boundaries can have any rate of twist, or pitch. The pitch is defined as the angle between a tangent to the curve and the tangent to the circle at that radius. The pitch is the same everywhere on a logarithmic spiral. Any such linear iterated function system (IFS) that includes scaling and rotation (an affine transformation) will contain logarithmic spiral patterns. Naturally, occurring algorithms (e.g. the expression of a genetic code, hurricane dynamics, and galaxy formation) commonly result in this shape. The shape also seems to be appealing to the eye, perhaps because our visual perception is tuned for interpreting similarity (scale and rotational invariance) of known objects.

Advantages of the logarithmic spiral

As sampling pattern method of the retinal image, the logarithmic spiral offers the following advantages:

1. The data dimensionality is reduced because the retinal vascular network is represented by a real valued data sequence [35].
2. The discontinuities are eliminated in the data caused by sampling, which occurs when concentric flatted circles or other sampling methods are used. The connectivity is a concept geometrically intuitive: A set is connected if it is composed of a single segment. Tuning the initial concept has come to define the connectedness paths: A set C is connected by road from any point x if the same can reach any point C and touring a "continuous path" that does not leave the set. We must recall that a connected component is a set of pixels such that for any pair of pixels on the whole, there is a digital path that connects them. Intuitively, a connected set is that composed of a single 'piece', which cannot be 'split' into parts [38].
3. Only the points of the vascular network detected by the spiral are encoded and not the entire region which includes the background; the features are extracted only

along the spiral path. For every point P in the spiral certain structural information at P is used as the feature [37].

4. A single sample for each point and a single sequence for each kind of coded data are provided [37].
5. Travel and distribute in the same way as the vascular network does: in geometric progression. The most problematic area is located within the optical disc which we had removed previously.
6. The most robust and stable structure of the image is coded, that is, the vessel segments of the vascular network and not to the branches, crossings and ending points. Bifurcations and crossings are eliminated in order to avoid coding errors [28-32].
7. It is not necessary to specify whether a given vessel is a vein or an artery, because the midpoint of every detected vessel segment is used as the feature descriptor.
8. The amount of coded information is increased because it is possible to extract some other features from the detected vessels along the spiral path [37].
9. The required size of the spiral or the number of turns is determined by the number of the necessary points that ensure the subject's individuality [36]. This provides invariance to small changes in the scale.

DRIVE Database

In this paper we used the images included in the publicly available DRIVE database [17], to implement the proposed method and to assess its performance. It consists of 40 color retinal images of size 565 × 584 pixels with 8 bits per color channel. The File of View (FOV) is circular with approximately 535 pixels in diameter. For each image, a mask image is provided that delineates the FOV. Hence, detection of the FOV border is not needed in this case. Images have been divided into 2 sets: a training set and a test set, each containing 20 images. The training set is useful to design supervised segmentation methods. Those images of the test set were segmented twice, resulting in a set A and a set B. In set A, 12.7% of pixels were marked as vessel, against 12.3% for set B. Performance is evaluated on the test set using the segmentations of set A as ground truth. All images were manually segmented.

The proposed method

As depicted in Fig. 2, the proposed methodology is composed of two main processing stages. In the next section we discuss each stage in detail.

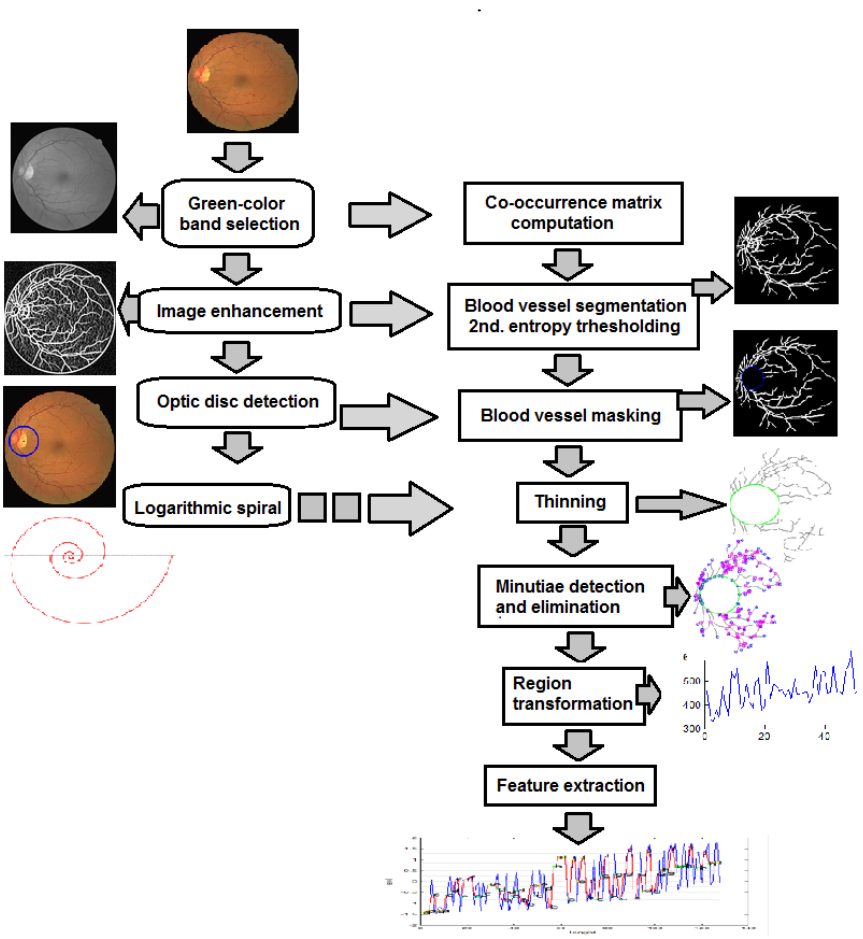

Fig. 2 Block diagram of the proposed method

1. Preprocessing stage: This step permits us to obtain the blood vessel image segmented from the original gray scale retinal image and thus, the minutiae feature extraction task is simplified. The preprocessing step consists of the following 4 stages: a) green-color band selection, b) image enhancement for vessel network detection, c) optic disk detection, and d) logarithmic spiral creation.

2. Main processing stage: This issue constitutes the essence of an automatic biometric authentication system design and has far reaching implications on the performance of the rest of the system. The main process consists of 7 stages: a) co-occurrence matrix computation, b) vessel segmentation by the second entropy thresholding technique, c) blood vessel masking in the vicinity of the optic disc, d) morphological thinning of the network, e) landmarks detection for their elimination, f) rectangular region transformation into sequential data, and g) time series creation that represent the features.

Preprocessing stage

Preprocessing of the retinal image is a requirement after image acquisition due to the high variability of this process. The preprocessing stage is also required to obtain a better and a more homogeneous representation of the retinal image in order to achieve repeatability in the feature extraction stage [10]. Preprocessing of retinal image is necessary to: [15]

- Improve the contrast of blood vessel structures;
- Maintain their integrity;
- Avoid introduction of spurious structures or artifacts; and
- Retain the connectivity of the blood vessels while maintaining separation between them.

2.0.1 Green-color band selection

A gray-level image is obtained by extracting the green layer from the original RGB image. The green component has the blood vessels on a highly contrasted background (dark blood vessels on a relatively bright background). Hence, the green channel of image is preferred for the retinal vasculature detection [2] [16].

2.0.2 Image enhancement

Image denoising and contrast enhancement are needed before applying the vessel segmentation algorithm for landmark extraction. Uneven illumination (also called shading) is present in retinal images and must be suppressed in order to achieve more accurate segmentation of the blood vessels. In order to characterize the retinal features of interest, we use a Gaussian matched filter (GMF) to detect piecewise linear segments of blood vessels in retinal images [18].

2.0.3 Optic Disc Detection

The optic disk is the brightest area in images that have not large areas of exudates and it is a slightly oval disk. It is the entrance region of vessels and its detection is very important since it works as a landmark for the other features in the retinal image. Hence, by targeting common structures such as the optic disc and the retinal vascular branches, a consistent source of readily identifiable, yet contrasting structures are available for digital imaging and processing. The entrance point of the optic nerve itself is taken as a point of reference. The distances and directions of the vein forks from this reference point provide coordinates which can be hooked together in a serial number for classified filing and quick comparison.

In the preprocessing technique used to detect the optic disc, the blood vessels are “erased” from the original retinal fundus image through the successive application of two morphological operations with a disk-like structuring element with N pixels radius. First, it is used a morphological opening operation. The circled structuring element is applied on the green color band of the fundus image. Next, it is used a

morphological closing operation employing the same circled structuring element, which is applied to the resulting image obtained from the previous step operation. Then, the resulting image becomes a binary mask by means of a thresholding scheme, which uses the Matlab function "IM2BW" found in the library of the image processing Toolbox. The threshold value *h* is computed by using the Matlab function "GRAYTHRESH" included in the same Toolbox. After this, the obtained binary image is labeled. The area of the labeled regions in the binary image is calculated and the region with the greatest area is isolated, which corresponds to the optic disc. Finally, we compute the coordinates of the centroid of this isolated region to be used as the reference point [16].

The experiment results of the preprocessing step of our algorithm are illustrated in Fig. 3. Fig. 3 a) shows the original image used to illustrate the accurate detection of the optic disc location. Fig. 3 b) illustrates the origin of the detected location of the optic disc indicated by a blue asterisk surrounded by a circle of the same color.

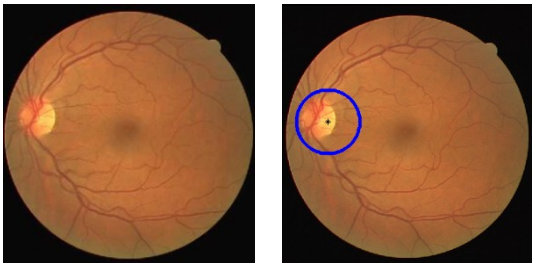

a) b)

Fig. 3 Experimental results of the optic disc detection step for a typical image. a) Original image, b) optic disc detected

2.0.4 Logarithmic spiral creation

We create the logarithmic spiral (Fig. 4) starting from the center of the optic disc (used as the origin of the logarithmic spiral path) by using the Eq. 1.

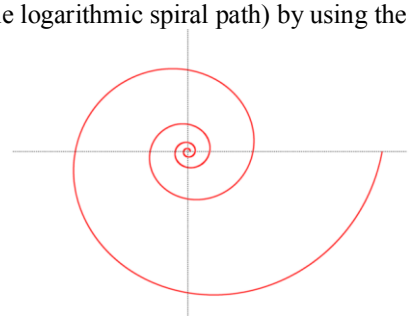

Fig. 4 Logarithmic spiral

Main Processing stage

To characterize the searched retinal features, it is necessary a good image preprocessing. Therefore, the propose method detect vessels using the knowledge of their known gray level profile and the concept of the matched filter detection, which is used to detect piecewise linear segments of blood vessels in retinal images.

2.1.1 Gaussian matched filter

A matched filter is constructed for the detection of the vessel edge segments searching in all possible directions [19]. A Bell-Shaped Gaussian matched filter (BSGMF) was developed to cover all 12 orientations where designed kernel is given by Eq. 2.

$$K(x,y) = \pm \left(\quad \right) \qquad \text{(Eq. 2)}$$

The application of this method enhances individual vessels segments in the image. A proper thresholding scheme must be used to distinguish between the enhanced vessel segments and the background.

2.1.2 Second-entropy thresholding segmentation method

The proposed segmentation thresholding method exploits the entropy of the distribution of the gray levels in the image. The maximization of the entropy (Eq. 3) of the thresholded image is interpreted as indicative of maximum information transfer [22], [23], [24]. In Figure 5 some examples of the segmented blood vessels, using the 2nd local entropy thresholding method are presented.

$$t_{LRE} = \max_{t \in [\quad]} J(t) \qquad \text{(Eq. 3)}$$

2.1.3 Blood vessel masking

Eventually, the edge of the optic disc could be misinterpreted by the segmentation method as a blood vessel, therefore, it is necessary to delete or hide this area to reduce the errors that its structure may cause.

In order to remove the blood vessels within the region of the optic disc, we superimposed a disc-shaped binary mask with a radius r_1 10% greater than the radius of the optic disc centered at optic disc location. It is possible to do so when we can assure that all images are of the same size. Two examples of the blood vessel erased images are shown in Fig 5.

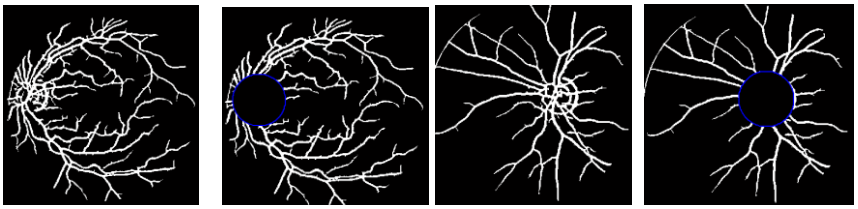

Fig. 5 Results of the erasing blood vessels in the vicinity of the optic disc

2.1.4 Morphological thinning

Vessels in the vicinity of the optic disc have different diameter size. To overcome this, retinal vessel thinning (through a skeletonizing method) is usually implemented using a morphological operator that reduces the width of vessels to a single pixel width line segments while preserving the extent and connectivity of the original shape. The thinned representations is typically easier to process in later stages producing savings in both time and storage complexity [25].

2.1.5 Minutiae extraction for their elimination

The bifurcation points in the thinned vessel tree are detected using the crossing number method [26] and then erased, thus only the vascular structure of the vessel segments is retained.

2.1.6 Rectangular region transformation

In order to represent the retinal vascular network using a time series, the rectangular region with the skeletonized vascular network must be transformed into sequential data. There are many possible ways of decomposing a 2D image into sequential data. In this work, we adopted a logarithmic spiral as the track for the decomposition. Thus, only this region is sampled with the logarithmic spiral, starting from the external edge of the masked optic disc towards the periphery of the vascular network.

2.1.7 Feature extraction and representation

For each point on the spiral, the position and angle of the midpoint of the blood vessel segments are encoded and a time series is created for each descriptor, one time series for the position and one time series for the angle. Figure 6 show both time series of a typical coded retinal image using a logarithmic spiral with a parameter $a = 0.15942$.

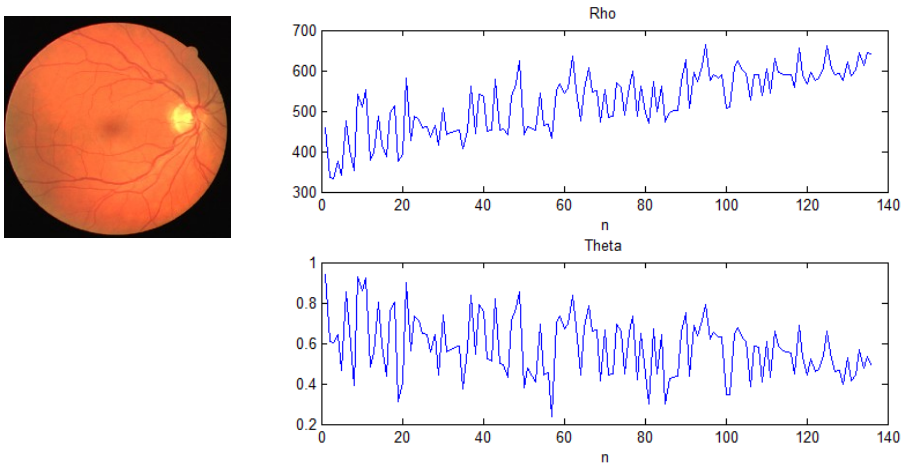

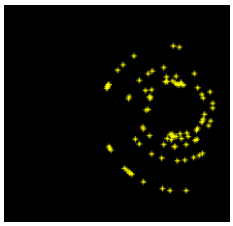

Fig. 6 Time series with a = 0.15942

All the steps mentioned above are repeated using different parameter values of the logarithmic spiral equation (*a* and *b*) in order to analyze the behavior of the generated biometric code.

2.1.7.1 *SAX Representation*

Dimensionality reduction is achieved by converting time series into its SAX representation Qsax [27]. We first transform the time series into the Piecewise Aggregate Approximation (PAA) representation and then symbolize it as a discrete string. The PAA representation is merely an intermediate step required to obtain the symbolic representation, to be transformed later in the SAX discrete sequence, Q_{SAX}. The number of segments and levels of the Q_{SAX} can be used to control the degree of the dimensionality reduction (See figure 7).

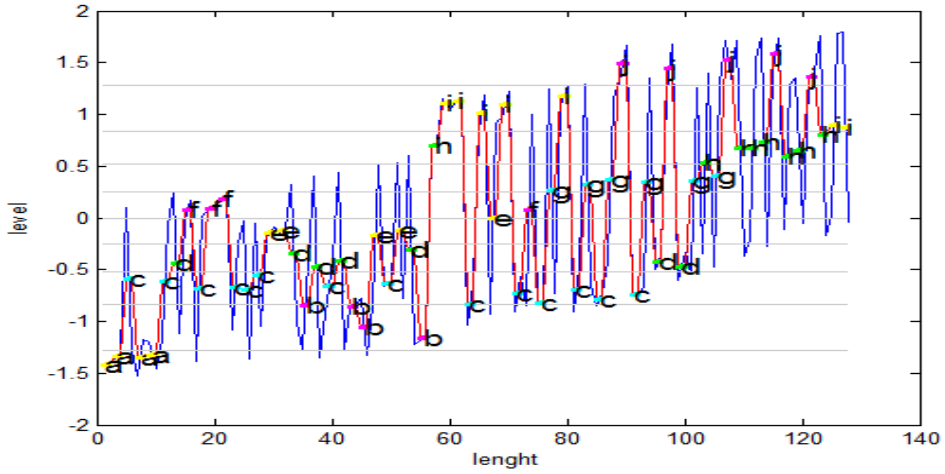

no. Seg = 64;
data length = 10;

'a'	'a'	'c'	'a'	'a'	'c'	'd'	'f'	'c'	'f''	'f'	'c'	'c'	'c'	'e'	'e'	'd'
'b'	'd'	'c'	'd'	'b'	'b'	'e'	'c'	'e'	'd'	'b'	'h'	'i'	'i'	'c'	'i'	'e'
'i'	'c'	'f'	'c'	'g'	'i'	'c'	'g'	'c'	'g'	'j'	'c'	'g'	'd'	'j'	'd'	'g'
'h'	'g'	'j'	'h'	'h'	'h'	'j'	'h'	'h'	'j'	'h'	'i'	'i'				

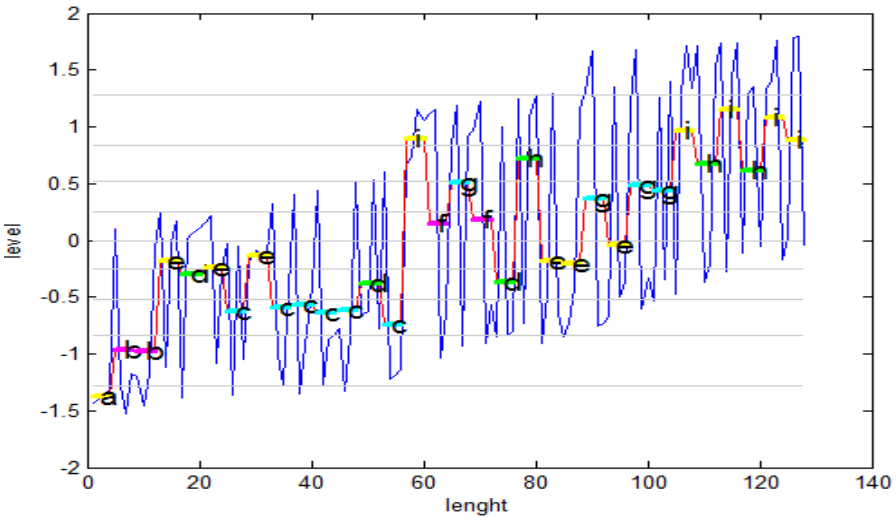

No. seg = 32;
Data length = 10;

'a' 'b' 'b' 'e' 'd' 'e' 'c' 'e' 'c' 'c' 'c' 'c' 'd' 'c' 'i' 'f' 'g'
'f' 'd' 'h' 'e' 'e' 'g' 'e' 'g' 'g' 'i' 'h' 'i' 'h' 'i' 'i'

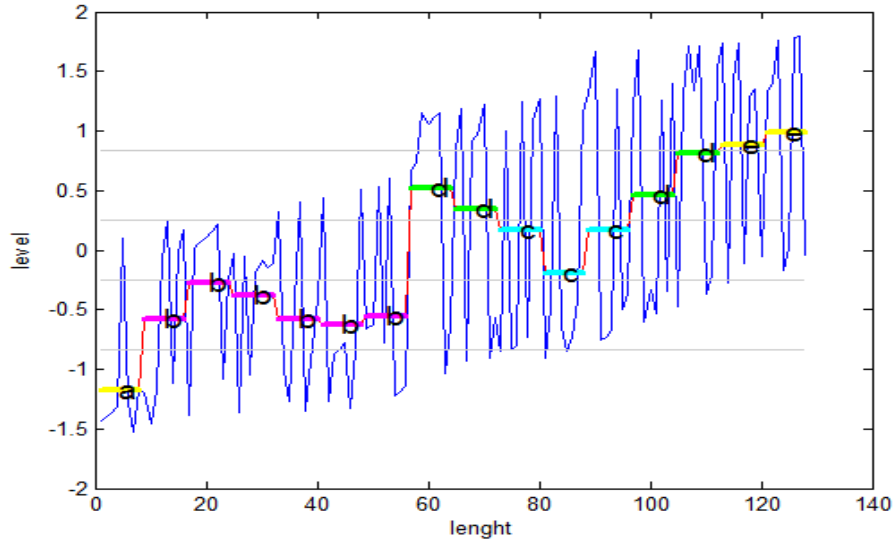

No. seg = 16;
Data length = 5;

'a' 'b' 'b' 'b' 'b' 'b' 'b' 'd' 'd' 'c' 'c' 'c' 'd' 'd' 'e' 'e'

Fig. 7 Three SAX representations and data sequences of the same retinal image with different parameters

Fig. 7 shows some examples of the extracted data sequence and the corresponding SAX representations with different lengths and levels illustrated in a typical retinal image. The SAX representation Qsax is used as the template of the retinal vascular network.

Experimental results

In this section we present our experimental results on the performance of the proposed blood vessel segmentation method and of the feature extraction scheme. The blood vessel segmentation and feature extraction approach introduced in the last stages of the system will be evaluated to verify the suitability of such proposal.
The first stage of the evaluation is the blood vessel segmentation method. The second part of the experiment will be focused on testing the feature points extraction step.

Blood vessel segmentation performance

The proposed segmentation method was applied to all 20 images of the training set of the DRIVE database, and TPR (true positive rate) and FPR (false positive rate) metrics were computed using the mask images provided by the database. A pixel-by-pixel comparison between the outcome images and the ground truth was made. The algorithm in the presented form yielded a TPR for these 20 images of 0.95356726 with a FPR of 0.00352145. The experimental results show that the proposed method performs well in extracting vessels. There are several parameters of the algorithm that have effects in the performance of the vessel segmentation method. The most significant parameter is the thresholding value. Since the proposed segmentation method obtains automatically this value for each image, it is not necessary to establish a range of thresholding values, and also, the interaction of the user to adjust this value depending on the image case is not necessary.

Feature extraction performance

To adjust the parameters and evaluate the methodology of using encryption as a logarithmic spiral sampling pattern, we implemented the sequence of steps presented above and analyzed the results obtained for each image and for each value used in the implementation parameters. Table 1 shows the minimum, maximum and average number of detected points and the required computational time depending on the rotation value of the logarithmic spiral in all analyzed database.

From the results it is possible to observe the inverse relationship between the logarithmic spiral turn and the amount of encoded points, i.e., when this value is small, the resulting spiral travels very gently, so that the number of turns is greater and therefore, the number of points that can be detected increases, but also greatly increases the required time to generate the time series.

The obtained results using the complete database allow us to establish a more realistic picture about the average number of detected points for a given rotation value of the

spiral. In this way we could estimate the better rotation value to ensure that the number of detected spots for all images is considered adequate to establish the individuality of the person. As a result, the subject could be positively identified using this biometric template without sacrificing the efficiency of the system and without increasing significantly the processing time.

For example, if we choose a rotation value of 0.05 for the logarithmic spiral, the average number of coded points will be 125, and the time that the system need to encode an image would be 2.22 s.

Table 1. Max, min and average number of detected points and the required computational time according to the rotation value of the logarithmic spiral

Rotation value (°)	Max	Min	Mean	Time (s)
0.01	347	212	293	4.5
0.02	272	173	228	4.2
0.03	232	132	178	3.9
0.04	208	99	150	2.56
0.05	166	89	125	2.22
0.06	154	81	112	2.12
0.07	139	60	94	1.09
0.08	123	60	84	1.01
0.09	127	56	80	1.01
0.1	104	49	75	1.01
0.2	66	33	46	1.01
0.3	38	15	25	1
0.4	39	16	26	1
0.5	22	11	17	1
1	13	4	7	1
2	11	3	6	1

On the other hand, if we want to increase the number of coded points to 178, we must select as the spin value to 0.03, for which the system will take 3.9 s. This allows us to establish a range of allowed spin values, without increasing the processing times while ensuring the efficiency of the system and the individuality of the biometric code based on the logarithmic spiral.

From this analysis, we decided to select as the spiral value twist of 0.04, which guarantees to encode an average of 150 points in a time of 2.56 s.

Conclusions

We have proposed a novel approach for the retinal image coding using logarithmic spiral and time series technologies. Using a logarithmic spiral as the rectangular region decomposition method and the SAX tool for the template representation are the keys of this new approach. They have the following advantages: first, logarithmic spiral share the geometrical characteristics that retinal network has, it is simple to implement and the overall computational complexity is very low compared to previous works (for more details consult ref [37], Table 3); second, it is very flexible as the spiral parameters, the coded local features and the SAX parameters can be adjusted according to different system requirements; third, the SAX representation (essentially symbol string) makes it very convenient for the implementation of multi-biometrics using feature fusion; fourth, logarithmic spiral and SAX representation reduce the data dimensionality of the original retinal image to a real sequential data; fifth, reduce the computational time required for the template representation and the matching step.

Acknowledgements. The authors of this paper wish to thank the Center for Computing Research (CIC), Mexico; Research and Postgraduate Secretary (SIP), Mexico, National Polytechnic Institute (IPN), Mexico, and CONACyT, Mexico, for their support to this work.

References

[1] Keogh, E., Chakrabarti, K., Pazzani, M. & Mehrotra, S. (2001). Locally Adaptive Dimensionality Reduction for Indexing Large Time Series Databases. In *proceedings of ACM SIGMOD Conference on Management of Data*. Santa Barbara, CA, May 21-24. pp 151-162.

[2] Jung E. and Hong K., (2006). Automatic Retinal Vasculature Structure Tracing and Vascular Landmark Extraction from Human Eye Image, Proceedings of the International Conference on Hybrid Information Technology, IEEE Computer Society.

[3] Hill R. B., (1992). Retina Identification, Portland, OR, USA.

[4] Hill R.B., (1978). Apparatus and method for identifying individuals through their retinal vasculature patterns, U.S. Patent No. 4109237.

[5] Simon C., and Goldstein I., (1935). A new scientific method of identification. New York State. J. Medicine, 35(18):901-906.

[6] Tower P., (1955). The fundus oculi in monozygotic twins: Report of six pairs of identical twins. Arch. Ophthalmol., 54:225-239.

[7] Marshall J. and Usher D., (2006). Method for generating a unique and consistent signal pattern for identification of an individual, U.S. patent No. 6993161.

[8] Derakhshani R. and Ross A., (2007). A Texture-Based Neural Network Classifier for Biometric Identification using Ocular Surface Vasculature, Appeared in Proc. Of International Joint Conference on Neural Networks (IJCNN), Orlando, USA.

[9] Golden B. L., Rollin B. E., Switzer JR. R. V., (2004). Apparatus and method for creating a record using biometric information, U.S. Patent No. 028343.

[10] Ortega M., Gonzalez M.F., (2009). Automatic system for personal authentication using the retinal vessel tree as biometric pattern, PhD. Thesis, Department of Computer Science of the Faculty of Informatics of the University of Coruña downloaded from: http://www.varpa.es/. (Revised on June 10, 2012.)

[11] http://www.absoluteastronomy.com/topics/Retinal_scan. (Revised on June 10, 2012.)

[12] Bevilacqua V., Cambó S., Cariello L., Mastronardi G., (2007), Retinal Fundus Hybrid Analysis Based on Soft Computing Algorithms, Communications To Simai Congress, ISSN 1827-9015, Vol. 2.

[13] Usher D., Tosa Y. and Friedman M., (2007). Ocular Biometrics: Simultaneous Capture and Analysis of the Retina and Iris, Advances in Biometrics Sensors, Algorithms and Systems, pp. 133-155.

[14] Usher D.B., (2003). Image analysis for the screening of diabetic retinopathy, PhD thesis, University of London.

[15] Keisuke Fukuta; Toshiaki Nakagawa; Yoshinori, Hayashi; Yuji Hatanaka; Takeshi Hara; Hiroshi Fujita, ((2008), Personal identification based on blood vessels of retinal fundus images (Proceedings Paper), Medical Imaging, Image Processing, Proceedings Vol. 6914.

[16] Lee S. S., Rajeswari M., Ramachandram D., Shaharuddin B., (2006). Screening of Diabetic Retinopathy - Automatic Segmentation of Optic Disc in Colour Fundus Images, Proc 2nd International Conference on Distributed Frameworks for Multimedia Applications, pp. 1-7.

[17] http://www.isu.uu.nl/Research/Databases. (Revised on September 20, 2012)

[18] Choe T.E., Cohen I., Lee M. and Medioni G., (2006). Optimal Global Mosaic Generation from Retinal Images, the 18th International Conference on Pattern Recognition.

[19] Chaudhuri S., Chatterjee S., Katz N., Nelson N. and Goldbaum M., (1989). Detection of Blood Vessels in Retinal Images Using Two-Dimensional Matched Filters, IEEE Transactions on Medical Imaging, 8(3):263–269.

[20] http://mathworld.wolfram.com/LogarithmicSpiral.html. (Revised on September 20, 2012)

[21] http://www.2dcurves.com/spiral/spirallo.html. (Revised on September 20, 2012).

[22] Zhang Y. F, and Zhang Y, (2006). Another Method of Building 2D Entropy to Realize Automatic Segmentation, International Symposium on Instrumentation Science and Technology; Journal of Physics: Conference Series 48, 303–307.

[23] Kullback, S., (1977). Information theory and statistics, Communications and Information Theory, Vol. 1, Issue 4, pp. 417 – 528.

[24] Pal N.R. and Pal S.K., (1989). Entropic thresholding, Signal Process, 16, 97-10.

[25] Bevilacqua V., Cambo S., Cariello L. and Mastronardi G., (2007). Retinal Fundus Hybrid Analysis Based on Soft Computing Algorithms, Communications To Simai Congress, ISSN 1827-9015, Vol. 2.

[26] Wu C., (2007). Advanced Feature Extraction Algorithms for Automatic Fingerprint Recognition Systems, a Dissertation submitted to the Faculty of the Graduate School of State University of New York at Buffalo in Particular fulfillment of the requirements for the degree of Doctor of Philosophy.

[27] J. Lin, E. Keogh, S. Lonardi, B. Chiu, (2003). A Symbolic Representation of Time Series, with Implications for Streaming Algorithms., Proceedings of the 8th ACM SIGMOD Workshop on Research Issues in Data Mining and Knowledge Discovery, San Diego, CA. pp. 2 -11.

[28] Zana F., Klein J.C., (1977), Robust Segmentation of Vessels from Retinal Angiography, International Conference on Digital Signal Processing, pages 1087–1091, Santorini, Greece.

[29] Zhoue L., Rzeszotarski M., Singerman L., Cokreff J., (1994), The detection and quantification of retinopathy using digital angiograms, IEEE Transaction on Medical Imaging: 13-4, 619-626.

[30] Matsopoulos G. K., Mouravliansky N. A., Delibasis K. K., Nikita K .S., (1999), Automatic retinal image registration Scheme using global optimization techniques, IEEE Trans. Information technology in biomedicine: 3.

[31] Wang L., Bhalerao A., (2003), Model Based Segmentation for Retinal Fundus Images, Proc. of Scandinavian Conference on Image Analysis (SCIA).

[32] H. Farzin, H. Abrishami-Moghaddam, M. Moin, (2008),A Novel Retinal Identification System", EURASIP Journal on Advances in Signal Processing, Article ID 280635, 10 pages, doi:10.1155/2008/280635.

[33] A. Arakala, J. S. Culpepper, J. Jeffers, A. Turpin, S. Boztas, K. J. Horadam, and A. M. McKendrick, (2009), Entropy of the Retina Template, ICB '09 Proceedings of the Third International Conference on Advances in Biometrics, Pages 1250–1259, ISBN: 978-3-642-01792-6.

[34] T. Fuhrmann, J. Hammerle-Uhl, and A. Uhl, (2009), Usefulness of Retina Codes in Biometrics, Advances in image and video technology, Lecture Notes in Computer Science, Volume 5414/2009, 624-632, DOI: 10.1007/978-3-540-92957-4_54.

[35] M. Z. Che Azemin, Dinesh K. Kumar and Hong Ren Wu, (2009), Shape Signature for Retinal Biometrics, 2009 Digital Image Computing: Techniques and Applications, DICTA'09, pgs. 382-386.

[36] http://www.biometricnewsportal.com/retina_biometrics.asp.

[37] Jiansheng Chen, Yiu-Sang Moon, Ming-Fai Wong, Guangda Su, (2010), Palmprint authentication using a symbolic representation of images, Image and Vision Computing 28 (2010) 343–351.

[38] http://en.wikipedia.org/wiki/Connected_space#Path_connectedness.